Available online at www.sciencedirect.com

SCIENCE DIRECT®

Catalysis Today 89 (2004) 455–464

CATALYSIS TODAY

www.elsevier.com/locate/cattod

Optimization of Cu oxide catalysts for methanol synthesis by combinatorial tools using 96 well microplates, artificial neural network and genetic algorithm

Yuhsuke Watanabe, Tetsuo Umegaki, Masahiko Hashimoto,
Kohji Omata, Muneyoshi Yamada*

Department of Applied Chemistry, Graduate School of Engineering, Tohoku University, Aoba 07, Aramaki,
Aoba-ku, Sendai 980-8579, Japan

Received 31 August 2003; received in revised form 24 December 2003; accepted 10 February 2004

Abstract

Compact and economic processes for methanol synthesis from syngas demand a new catalyst that is active under low-pressure and low temperature. Combinatorial approach comprising a high-pressure high-throughput screening (HTS) reactor system, an artificial neural network (NN), and a genetic algorithm (GA) was applied for the catalyst development. A variety of 96 microplates were used in the HTS reactor system for both preparation and activity testing to handle 96 catalyst samples simultaneously. Activity test results were used as training data for NN. After training, the NN can map catalyst activity as a function of catalyst composition and parameters for catalyst preparation. GA was used as an optimization tool to find maximum catalyst activity in the trained artificial neural network. Composition of methanol synthesis catalyst (Cu–Zn–Al–Sc–B–Zr), calcination temperature and the amount of precipitant were optimized simultaneously under pressure (1 MPa) because optimum catalyst composition is usually affected by both preparation and reaction conditions. The composition of the optimum catalyst was Cu/Zn/Al/Sc/B/Zr = 43/17/23/11/0/6 prepared using 2.2 times the equivalent of oxalic acid and calcined at 605 K. The activity (427 g-MeOH/kg-cat./h) was much higher than that of industrial catalyst (250 g-MeOH/kg-cat./h) at 1 MPa, 498 K.

Keywords: Methanol synthesis; Catalyst optimization; Combinatorial catalysis; Genetic algorithm; Artificial neural network

1. Introduction

Nowadays, dimethyl ether (DME) is synthesized from syngas (a mixture of CO, CO_2 and H_2) in a two-stage process in industry. In the first stage, a Cu-based oxide catalyst is used for methanol synthesis from syngas; in the second stage, a solid acid catalyst is used to dehydrate methanol to produce DME. The production scale is usually very small because DME is used mainly as a non-CFC propellant for spray cans. Recently, DME has attracted much attention as an important candidate for a diesel fuel alternative because emission of NO_x, SO_x and SPM, can be improved when it is used as fuel in diesel engines instead of gas–oil. However, economic and efficient process is required for fuel use.

We propose a compact process to produce DME from dispersed unused carbon resources, such as small gas reservoirs or coal-bed methane. If the following are all achieved: (1) low-pressure-operation (ideally, 1–3 MPa), (2) high one-pass conversion (90% CO conversion), and (3) a one-stage reaction where hybrid catalyst of Cu-based oxide and solid acid is used, then both pressure compression of syngas and gas-recycling of unreacted syngas would be omitted. Through such a simple process, DME production costs would be reduced.

This study applied homemade combinatorial tools comprising automated catalyst preparation, high-pressure HTS reactor, and data mining tools to develop an active catalyst for low-pressure methanol synthesis. In order to attain high conversion under such a low-pressure, the catalyst must be operated under lower temperature because the synthesis of methanol and DME from syngas suffers from a severe equilibrium limit at lower pressure and higher temperature, as

---

* Corresponding author. Tel.: +81-22-217-7214;
fax: +81-22-217-7293.
E-mail address: yamada@erec.che.tohoku.ac.jp (M. Yamada).

0920-5861/$ – see front matter © 2004 Elsevier B.V. All rights reserved.
doi:10.1016/j.cattod.2004.02.001

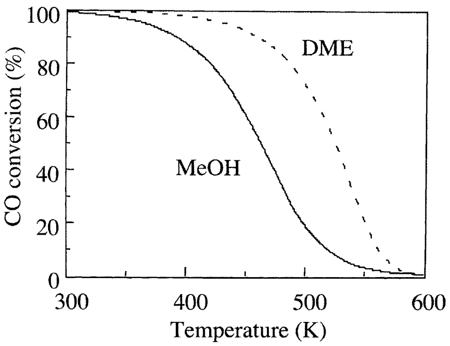

Fig. 1. Equilibrium conversion of methanol and DME synthesis from CO and H_2 at 1 MPa, H_2/CO = 2/1.

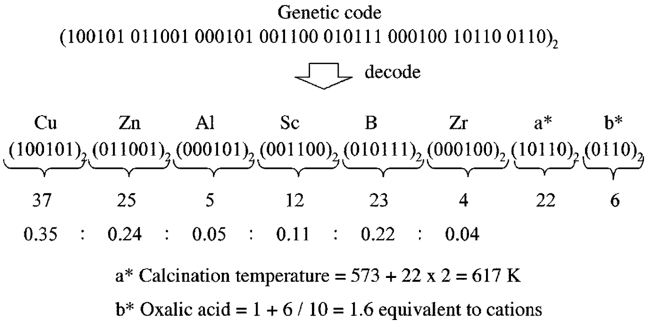

a* Calcination temperature = 573 + 22 x 2 = 617 K

b* Oxalic acid = 1 + 6 / 10 = 1.6 equivalent to cations

Fig. 3. HTS reactor with 12 parallel lines made by SUS 316. ID = 0.15 m, volume = 2.8 L. Reprinted from [5], Copyright (2000), with permission from the Japan Petroleum Institute.

shown in Fig. 1. Therefore, a new and highly active catalyst is needed because industrial methanol synthesis catalysts are not sufficiently active under these mild reaction conditions.

2. Methodology

Usually a combinatorial catalysis tool consists of combinatorial catalyst preparation, high-throughput screening (HTS), and informatics [1–18]. In development steps of our tools, a parallel reactor with 12 reaction lines was reported first to investigate the effect of Cu/Mn ratio for methanol synthesis under pressure (1 MPa) [5]. Twelve Swagelok "reducer"s were diverted to catalyst vessels and placed in a large autoclave, as shown in Fig. 2 [5]. In the next step, a genetic algorithm (GA) was applied to optimize the Cu-based oxide catalyst [11,15]; GA is widely used as a robust tool to perform optimization even without prior knowledge of the target. Because their affinity is high, the combination of HTS and GA with and without other evolutional method is often used for optimization of a heterogeneous catalyst [3–5,10,15].

The process of GA is a biological metaphor of natural evolution. Through natural evolution, genes are modified by selection, crossover and mutation. If a gene engenders high fitness to its environment by the modification, the probability of its survival is increased. As a result of accumulation of such small modifications, progeny genes differ from parents' by providing high fitness to an environment after a large number of process iterations, or generations. In our catalyst development, only a simple GA was used where the gene, fitness and environment corresponded to the catalyst (presented in binary code), activity, and reaction conditions, respectively. Fig. 3 shows the catalyst coding and decoding procedure in the GA program used in this study; a 45 bit binary code was used as a gene. Every catalyst component except for oxygen was expressed by 6 bits. After the binary codes of the first 36 bits (6 bits × 6 components) are converted to decimal numbers, the molar percentage of each component was calculated from the decimal number. Oxygen content was determined from stoichiometry. Thus, the (100101 011001 000101 001100 010111 000100) part in Fig. 3 is decoded to $Cu_{0.37}Zn_{0.25}Al_{0.05}Sc_{0.11}B_{0.22}Zr_{0.04}O_{1.23}$. As preparation parameters, the amount of precipitate (oxalic acid) and calcination temperature were coded according to Eqs. (1) and (2), respectively

$$\text{calcination temperature (K)} = 573 + (5\,\text{bits}) \times 2 \qquad (1)$$

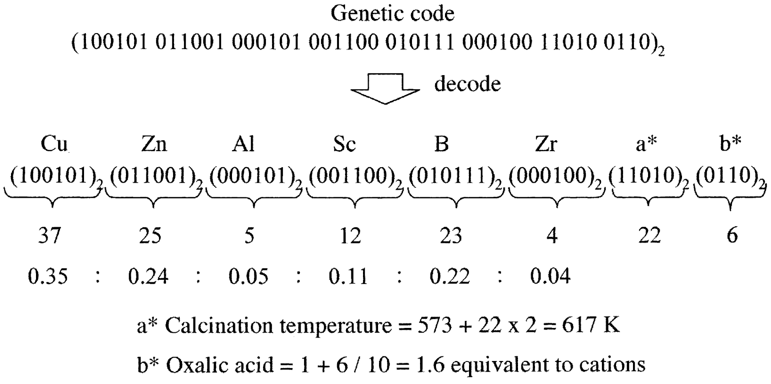

a* Calcination temperature = 573 + 22 x 2 = 617 K

b* Oxalic acid = 1 + 6 / 10 = 1.6 equivalent to cations

Fig. 2. Coding of catalyst composition and preparation parameters.

$$\text{precipitate (equivalent)} = 1.0 + \frac{4\,\text{bits}}{10} \qquad (2)$$

If the next 5 bits are (10110), as shown in Fig. 3, the calcination temperature is decoded as 617 K. The last 4 bits of the gene is code showing the amount of oxalate acid. If it is (0110), the precipitate of 1.6 equivalent to cations is used for catalyst preparation.

The 4320 bits (45 bits × 96) in 96 genes in the first generation were determined in a stochastic manner. Then the descending generation was decided by the GA program. The population was 96; therefore, 96 gene pairs were selected by the so-called “roulette rule” based on the fitness of the genes, namely activity of the catalyst, from the parent generation. Then 10% (=probability of crossover) of the pairs were selected stochastically and operated with one-point crossover where the two genes exchange their codes. After 96 genes were selected stochastically from the 192 genes, 1.5% (=probability of mutation) of all 4320 bits (45 bits × 96) were inverted as a mutation operation. The resulting 96 genes served as parents for the next generation. During these two operations, every bit of a gene was operated as an equivalent bit. Consequently, the GA program was very simple and was coded by a combination of internal functions on an Excel software spreadsheet [11].

Fitness of genes in a GA program is usually determined by experimental results. However, to replace laborious experimental steps such as catalyst preparation and activity test in the next step, evaluation by an artificial neural network (NN) was introduced in our combinatorial tool [14]. After NN is trained by experimental results, it can evaluate the gene fitness in the GA program. The network comprises an input layer, an association layer(s) and an output layer. Neurons in these layers are connected to all neurons in adjacent layers, but not to those in the same layer. Among many types of NNs, a back propagation network (BPN) was applied successfully to catalyst design; BPN is a supervised learning and feed-forward type network. It is modified by epoch-by-epoch backward calculation minimizing errors between the target and calculated data. For example, Hattori and Kito applied BPN for development of the catalyst for butane oxidation and oxidative dehydrogenation of ethyl benzene [19]. Hou et al. [20] and Huang et al. [21,22] used BPN to predict catalyst composition with high conversion and selectivity and developed catalyst performance. Corma et al. also used the combination of GA and NN [13]. The important checkpoint of BPN application is to avoid overtraining, which causes a loss of generalizability of the BPN. Optimization of BPN structure is necessary for that purpose. Aside from a trial-and-error method, many sophisticated procedures have also been developed [23,24].

Recently, radial basis function network (RBFN), a kind of NN, has also garnered much attention as an optimization tool in a variety of engineering fields because it is robust and suffers only slightly from over-training [25]. The apparent structure of RBFN is similar to BPN with only one hidden layer where a radial basis function is used instead of an S-shaped sigmoid function. During training, the center points of the radial basis functions are decided by training data; thus the input datum for RBFN is a vector. Then weights between the hidden layer and the output layer are determined to fit the output data to training data. We applied RBFN to evaluate gene fitness in the GA program. Optimization results were superior to those by the combination of BPN and GA [16,18].

The RBFN was constructed using STATISTICA Neural Network 6.0 (StatSoft). Normalized catalyst compositions of Cu/Zn/Al/Sc/B/Zr, calcination temperature and the amount of oxalic acid were given to the input layer and only STY (g-MeOH/kg-cat./h) issued from the output layer. The number of nodes in a hidden layer was set as identical to that of training data. We determined 190 catalyst parameters for RBFN training randomly, as described above. At first, 190 data were measured in an HTS reactor. Nevertheless, the number is insufficient to cover all combinations of parameters. When the resolution for the six components, the amount of oxalic acid, and calcination temperature are 1%, 0.1 equivalent, and 2 K, respectively, the total number of possible combinations is greater than 47 billion. Therefore RBFN was retrained using 234 data (original 190 data and additional 44 data) to improve the RFBN prediction accuracy. The 44 catalyst parameters were selected from developing generations and HTS reaction was performed to measure their activities.

Catalyst composition and preparation parameters were optimized simultaneously in this study using GA and RBFN. A new HTS reactor system using 96 well microplates [26] was also used both for preparation and activity testing to handle 96 catalyst samples simultaneously.

3. Experimental

3.1. Catalyst preparation

For industrial use, Cu–Zn oxide methanol synthesis catalysts are prepared using the alkaline co-precipitation method [27]. In this method, a highly active catalyst is obtained from highly dispersed Cu–Zn carbonate called Aurichalcite [28]. However, the method presents some difficulties, such as the need for delicate pH and temperature control; also, contamination of alkaline metals from precipitate should be avoided. On the other hand, it was reported that copper and zinc are easily dispersed by oxalate co-precipitation method [29]. Therefore, we employed the ethanol-oxalate method for catalyst preparation. For conventional activity testing, an ethanol solution of nitrates of Cu, Zn, Al, Sc, boric acid, and zirconium oxynitrate was mixed with a given composition; then an ethanol solution of oxalic acid was added to precipitate the mixed oxalic salts. The resulting mixed oxalates were washed with ethanol and dried at 353 K in vacuo. Oxalate precipitates were calcined at 593 K. Oxide precursors

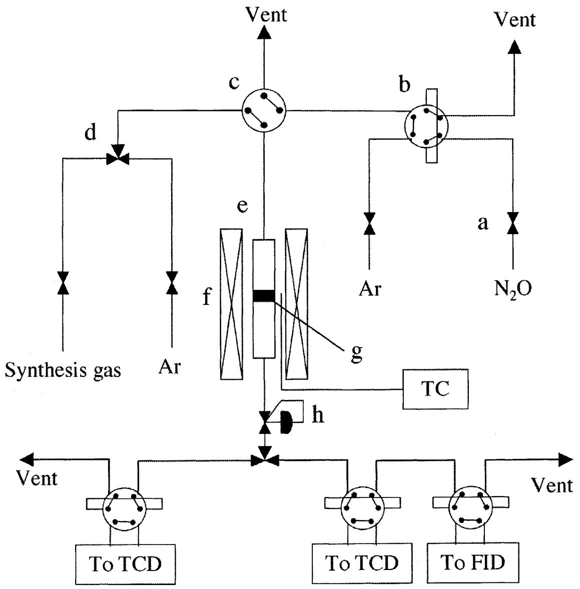

Fig. 4. Fixed bed reactor for methanol synthesis and in situ N_2O titration: (a) stop valve, (b) six-way valve, (c) four-way valve, (d) three-way valve, (e) reactor, (f) electric furnace, (g) catalyst, (h) back pressure regulator.

were packed into a SUS reactor after being sieved. Oxide precursor was reduced using synthesis gas before the reaction.

Catalysts for HTS were prepared according to a similar method using 96 well microplates. In this case, each catalyst composition was determined randomly. All solutions were dispensed into 96 deep-well microplates (volume of each well was 2 ml) using liquid handler (222XL; Gilson Inc.). An ethanol solution of oxalic acid was added to each well. The amount of oxalic acid was selected randomly from 1.0, 1.5, 2.0, and 2.5 times the equivalent to total cation. The oxalate precursors were calcined at a temperature that was also randomly selected from 573, 593, 613, and 633 K. After weight measurement (15 mg), these oxide precursors were transferred into Durham tubes (OD 8 mm, 33 mm length) and reduced using synthesis gas.

3.2. Activity test

Two different apparatuses were used for the activity test: a conventional fixed bed reactor and an HTS reactor. Their flow sheets are shown in Figs. 4 and 5, respectively. The reaction gas comprises 60% H_2, 30% CO, 5% CO_2 and 5% Ar (as internal standard). Catalysts were activated by temperature-programmed heating up to 523 K under reaction gas flow. Reaction was performed at 498 K, 1 MPa, $W/F = 1$ g h/mol. Under these conditions, CO conversion is lower than equilibrium limit of methanol synthesis. Activity is shown as a space-time yield (STY, g-MeOH/kg-cat./h). In the conventional apparatus, CO conversion and methanol were analyzed by GC equipped with TCD and FID.

In HTS experiments, all catalysts were set into respective Durham tubes. Glass beads were packed in the bottom of the Durham tube. Two capillaries made of SUS (line A: ID 0.1 mm, 0.8 m length for gas purge at 0.1 MPa for catalyst pretreatment; line B: ID 0.1 mm, 11 m length for reaction at 1 MPa) were inserted in each bead layer. Catalyst was fixed above the glass beads layer by quartz wool. The 95 tubes with catalyst were arranged in an aluminum 96 well microplate, as shown in Fig. 6 [26]; one vacant tube at H12 position was used to check the background atmosphere. The whole aluminum plate with 96 Durham tubes was placed at the bottom of an autoclave. Reaction gas was introduced to each catalyst bed prior to reaction using line A to activate catalysts by temperature-programmed heating up to 523 K. *W*/*F* was below 1 g h/mol, where CO conversion is proportional to *W*/*F*.

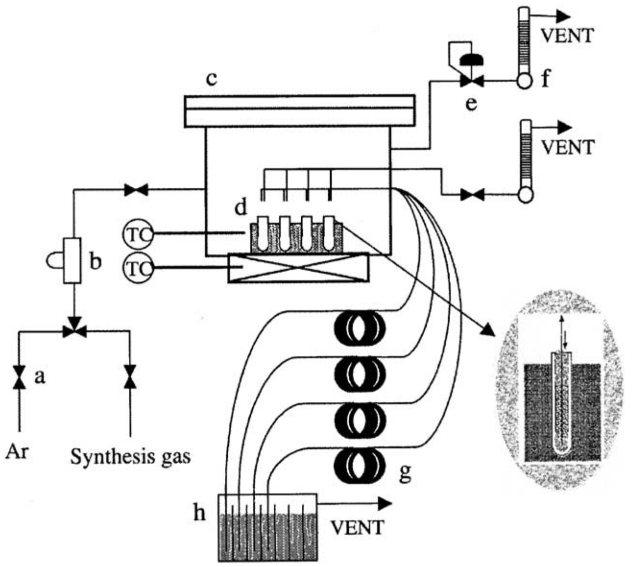

Fig. 5. HTS apparatus for methanol synthesis: (a) stop valve, (b) mass-flow controller, (c) autoclave, (d) aluminum block with Durham tube, (e) back pressure regulator, (f) soap flow meter, (g) SUS capillary tube, (h) water trap.

3.3. Parallel assay

For HTS reaction, parallel product assay is important. Color reaction was applied for quantitative analysis because the performance of GC, even rapid GC, is insufficient for 96 lines [26]. This type of assay is expected as real parallel analysis [30]. Produced methanol was depressurized through capillaries (line B) with syngas, and trapped for 3 h in water in a 96 deep-well microplate placed outside of the HTS reactor. Each methanol was detected by color reaction of dichromate, as shown in Eq. (3):

$$\begin{aligned}&3CH_3OH + K_2Cr_2O_7 + 4H_2SO_4 + 17H_2O\\&\quad\rightarrow 3CH_2O + 2KCr(SO_4)_2 \cdot 12H_2O \qquad (3)\end{aligned}$$

Potassium dichromate is reduced by alcohol to chrome alum. As shown in Fig. 7, chrome alum shows strong absorbance at 580 cm^{-1}. A microplate reader (595 and 655 nm filter,

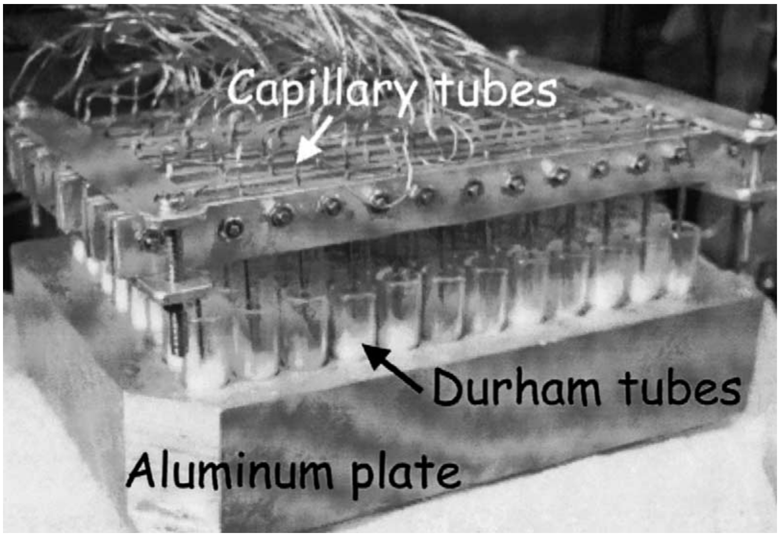

Fig. 6. Catalyst vessels arranged in aluminum 96 well microplate. Reprinted from [26], Copyright (2003), with permission from the Japan Petroleum Institute.

Model 550; Bio-Rad Laboratories, Inc.) was employed for quantitative analysis. Linearity of the calibration line is sufficient to measure STY of 15 mg catalyst, as shown in Fig. 8.

3.4. HTS reactor check

The HTS reactor system was subjected to test reaction. As shown in Fig. 9(a), the identical catalyst (Cu/Zn/Al = 6/3/1 M ratio) in 95 Durham tubes showed identical activity within experimental error. The activity was also identical to that in a conventional fixed bed reactor. Results supported the conclusion that aluminum block was effective for isothermal condition and that analysis using color reaction was consistent with that of the conventional GC analysis. In the next step, the catalyst (of another lot, Cu/Zn/Al = 6/3/1 M ratio) was placed in a checkerboard manner. The result in Fig. 9(b) reflects the lack of influence from adjacent tubes.

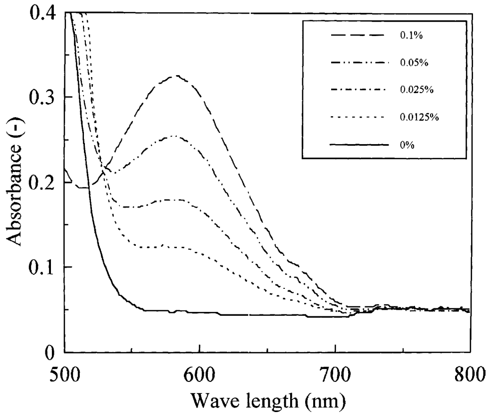

Fig. 7. UV-Vis spectrum change during color reaction by methanol. Shimadzu, UV-160, cell size: 1.2 mm × 1.2 mm × 4.5 mm. Reprinted from [26], Copyright (2003), with permission from the Japan Petroleum Institute.

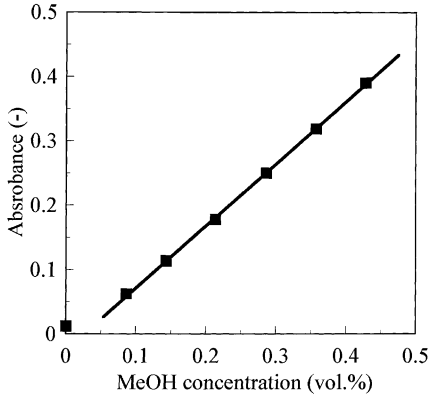

Fig. 8. Calibration of methanol concentration. Reprinted from [26], Copyright (2003), with permission from the Japan Petroleum Institute.

It was confirmed that all methanol formed in a Durham tube is certainly transferred to the corresponding well of the deep microplate connected by a capillary tube.

3.5. Characterization

Surface area was measured by nitrogen adsorption at 77 K (MS-19; Quantachrome Instruments). The surface area of metallic Cu after reaction was measured in situ in a fixed bed reactor (Fig. 3) by N_2O titration. Oxide structure was analyzed by XRD (Miniflex; Rigaku Co.).

4. Results and discussion

4.1. Selection of parameters

Whereas conventional or commercial Cu–Zn oxide catalysts are prepared using alkaline co-precipitation method,

(a) 96 lines check

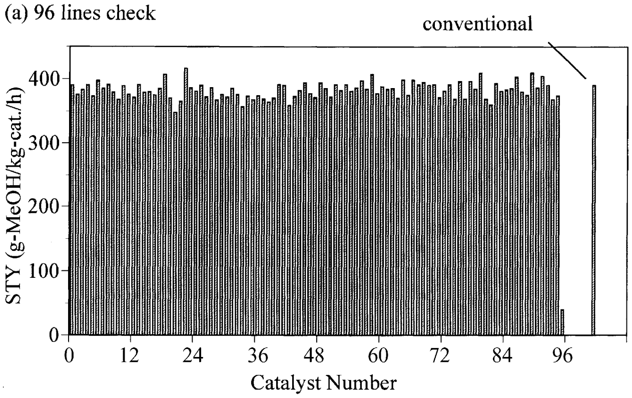

(b) Checkerboad patern check

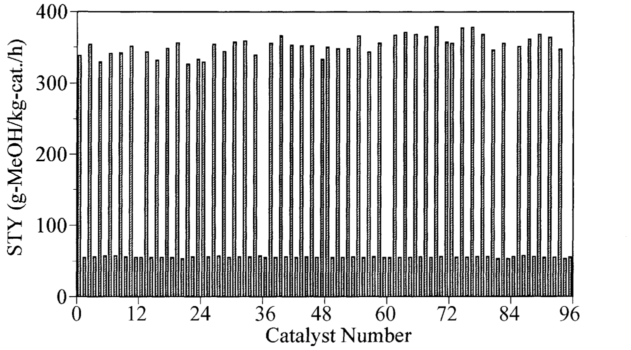

Fig. 9. Activity check for identical Cu–Zn–Al oxide catalyst at 498 K, 1 MPa. Reprinted from [26], Copyright (2003), with permission from the Japan Petroleum Institute.

other preparation methods for mixed oxides have been reported, such as ethanol-oxalate method, sol–gel method, and so on. Activities of Cu–Zn oxide catalysts prepared by these methods were compared [31]; that by ethanol-oxalate method showed the highest activity. This study used ethanol-oxalate method because highly dispersed Cu–Zn oxide can be obtained and contamination of precipitate can be prevented easily by this method.

The effect of additives was investigated to obtain high activity where Cu/Zn/X = 6/3/1 (X: additive, molar ratio). Fig. 10 shows the changes of surface area by N_2 adsorption and metallic Cu surface area obtained by N_2O titration by additives. Additives are indicated in the figure. Compared to Cu–Zn oxide without additive (shown as "None"), Li addition causes both low surface area and low metallic Cu surface area. The function is similar to that of Na, which promotes sintering of Cu [32]. Whereas Cr shows no effect, Al and Sc promotes both areas simultaneously. Ionic sizes of these additives very closely approximate that of Zn^{2+}; therefore, they are easily doped in ZnO lattice [33]. Excess electrons localized on the ZnO particles prevent aggregation of the particles to increase the surface area [33]. They were also found to have a synergistic effect on the activity of Cu–Zn–Al catalyst [18]. Boron was reported as an effective additive for methanol synthesis from CO_2. It escapes from the catalyst surface during reaction to expose a new active site resulting in higher activity [34]. Our observation corresponds to the mechanism. Boron only increases metallic Cu surface area and gives higher STY, as shown in Fig. 11 where the effect of these additives on activity is plotted as a function of metallic Cu surface area. The synergistic effect of B and Zr is expected because Zr increases only surface area, unlike B. As shown in Fig. 11, STY is proportional to the metallic Cu surface area in accordance with the report that active site is Cu metal when CO_2 is contained in the feed syngas [35]. Al, Sc, B, and Zr were selected as optimization targets.

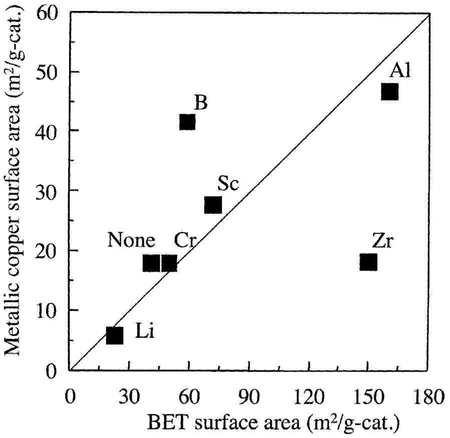

Fig. 10. Relationship between BET surface area and Cu surface area at 1 MPa, 498 K, $W/F = 2$ g h/mol.

At the last stage of ethanol-oxalate method, the precipitated mixed oxalate is converted to mixed metal oxide by calcination according to Eq. (4)

$$M(COO)_x \rightarrow \frac{1}{2}MO_x + \frac{1}{2}(x)CO + \frac{1}{2}(x)CO_2 \qquad (4)$$

It is possible that CO from precursor reduces CuO or Cu_2O immediately after its formation and Cu sinters easily at high temperature [36]. Both decomposition temperature and decomposition atmosphere are important factors for high activity because thermal stability of Cu metal is insufficient.

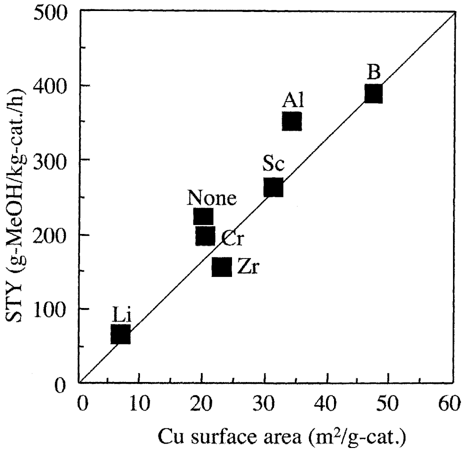

Fig. 11. Influence of additives on the relationship between STY and Cu surface area at 1 MPa, 498 K, $W/F = 2$ g h/mol.

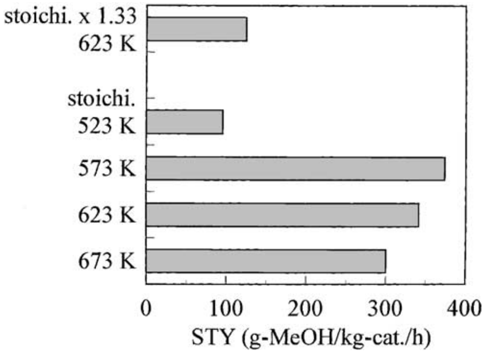

Fig. 12. Effect of calcination temperature on catalytic activity of methanol synthesis at 1 MPa, 498 K. Reprinted from [31], Copyright (2002), with permission from Elsevier.

The effect of calcination temperature is shown in Fig. 12 [28] where Cu/Zn/Al = 6/3/1 and the equivalent amount of oxalic acid were used for precipitation. The catalyst obtained by 573 K calcination shows the highest activity. XRD patterns of these oxides are illustrated in Fig. 13. Sintering of Cu and Zn oxides is observed, whereas at 523 K decomposition of oxalates does not proceed [31]. Furthermore, the difference in size and shape of clucibles influence the circulation of gas inside the crucible set in a furnace. Therefore, degree of Cu sintering by CO formed by oxalate precursor decomposition should be different.

Aside from the calcination temperature, effects of the amount of oxalic acid were investigated as shown in Fig. 14. Contrary to the catalytic activity, BET surface area of oxide precursors increases when the quantity of oxalic acid increases. Such contrariety can be explained from a viewpoint of Cu stability: because methanol synthesis reaction is exothermic reaction, Cu may sinter easily, if reduction and reaction start-up by pressurizing and/or temperature raising are too rapid, by overheating of catalyst bed. In order to elucidate this point, the effect of start-up temperature was examined in the following manner. Catalysts were reduced by temperature-programmed heating up to the star-up temperature under 0.1 MPa, then catalyst bed was pressurized up to 1 MPa followed by temperature tuning to 498 K. Afterwards, activity was compared at 498 K (Fig. 15). The catalyst prepared using twice equivalent oxalic acid showed higher activity when the start-up temperature is low. Clearly, the use of excess oxalic acid produces an active but thermally sensitive catalyst. Overall, we inferred that a balance of parameters for high-activity and for high-stability is important: simultaneous optimization is needed for both catalyst components (Cu, Zn, Al, Sc, B, Zr) and preparation conditions (amount of oxalic acid and calcination temperature).

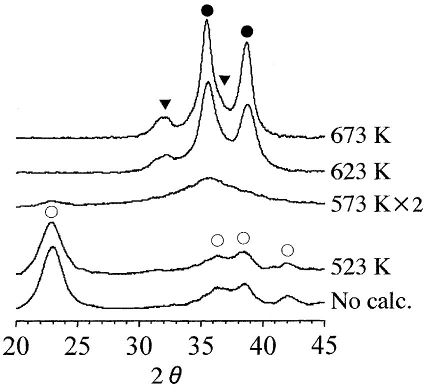

Fig. 13. Effect of calcination temperature on X-ray diffractogram. Copper oxalate (○), copper oxide (●), and zinc oxide (▼). Reprinted from [31], Copyright (2002), with permission from Elsevier.

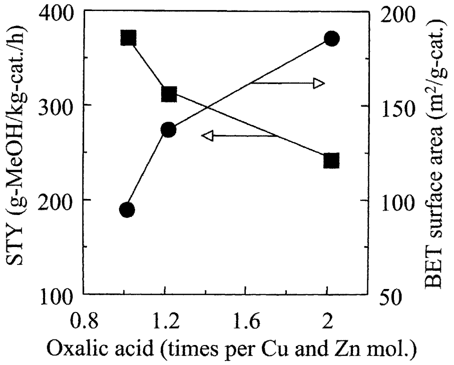

Fig. 14. Effect of amount of oxalic acid on BET surface area and STY.

4.2. HTS and data mining

Activity tests of 190 random catalysts were performed in the HTS reactor. Fig. 16 shows the observed activities. It is not so difficult to visualize the relation between the parameters and activity to find the optimum directly if there are few independent parameters. However, eight parameters must be optimized in this study. So RBFN was applied to obtain useful and quantitative information from these data. After the RBFN was trained successfully using the 190 data in Fig. 16, observed activities were mapped as a function of catalyst composition, the amount of oxalic acid, and calcination temperature. Hereafter, the RBFN works as a subroutine in the GA program to output the fitness of genes.

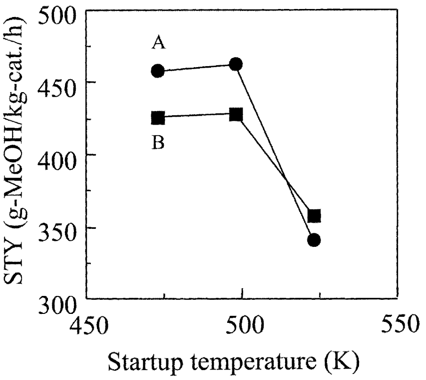

Fig. 15. Effect of start-up temperature on methanol synthesis activity: (A) two times excess; (B) equivalent molar of oxalic acid.

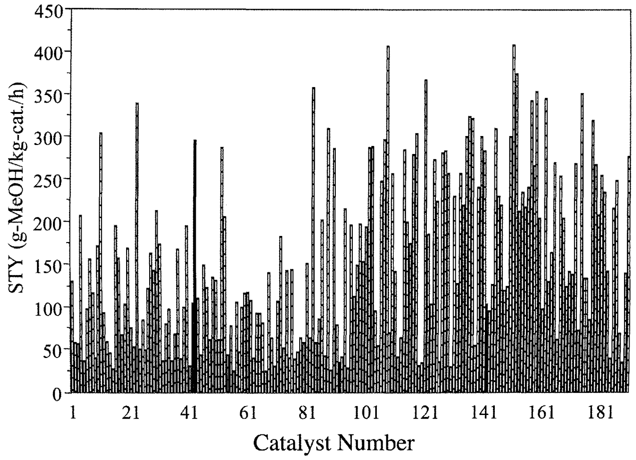

Fig. 16. Results of HTS experiments at 1 MPa, 498 K, $W/F < 1$ g h/mol.

Generation alternation was repeated based on the trained RBFN. That optimization process is shown in Fig. 17. The activity is illustrated as a function of main components (Cu and Zn). At the 80th generation, the maximum STY is 519 g-MeOH/kg-cat./h. From the history of the maximum value and dispersion of parameters, the maximum point was considered to be the point of convergence where Cu/Zn/Al/Sc/B/Zr = 38/24/32/1/0/5, 1.6 times the equivalent oxalic acid and calcination at 617 K. Experimental results showed, however, that the real STY of the catalyst was 390 g-MeOH/kg-cat./h.

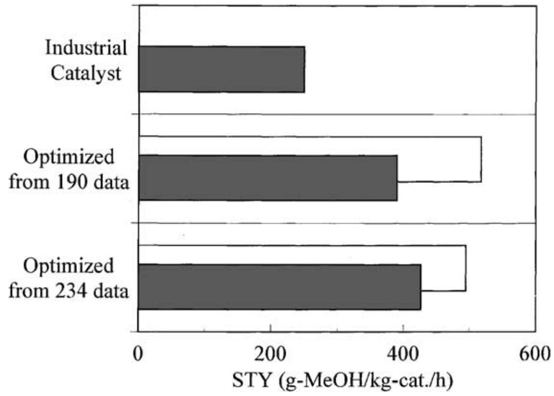

Fig. 18. Comparison of activity at 1 MPa, 498 K. White and black bars show predicted and experimental STY, respectively.

As mentioned in Section 3, the difference probably results from insufficient information around the optimum point. Corma et al. reported that the precision of prediction of back propagation network (BPN) based on GA increased with increasing of the number of training data [13]. In that case, HTS was repeated after every generation alternation to accumulate the training data. Instead, in this study, additional 44 training data of active catalysts in the former generation were collected by HTS. RBFN was then retrained again using all 234 data. Based on the retrained RBFN, generation alternation was repeated until the 90th generation to find the maxima. The maximum STY was predicted to be 495 g-MeOH/kg-cat./h by Cu/Zn/Al/Sc/B/Zr = 43/17/23/11/0/6, 2.2 equivalent oxalic acid and calcination at 605 K. The real STY was determined by experimentation to be 427 g-MeOH/kg-cat./h. Therefore, prediction was achieved further by additional semi-optimized data.

These activities are compared with that of the industrial catalyst in Fig. 18. That comparison shows clearly that the

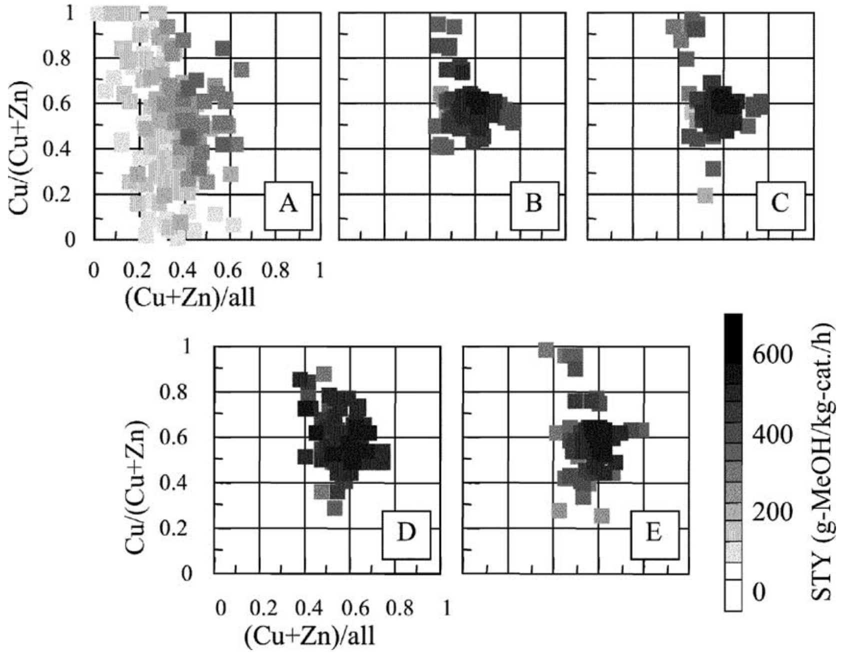

Fig. 17. Optimization process by GA based on RBFN: (A) first generation, (B) 20th generation, (C) 40th generation, (D) 60th generation, (E) 80th generation.

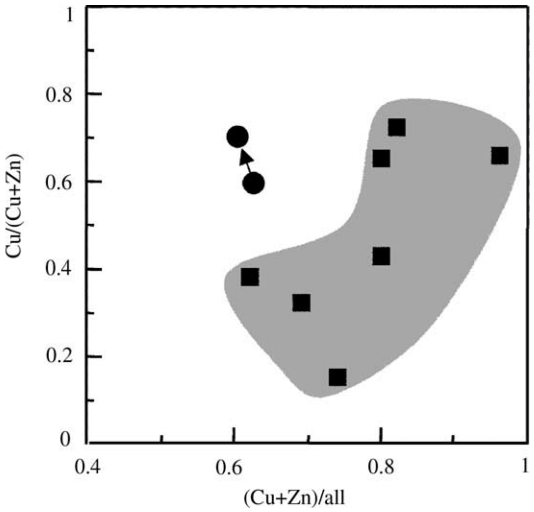

Fig. 19. Comparison of catalyst composition. Optimized catalyst (●), industrial catalyst (■).

optimized catalyst is superior to an industrial one. This superiority of the optimized catalyst is reasonable because industrial catalysts are optimized to different reaction conditions (i.e. higher pressure (5–10 MPa), higher temperature (503–523 K) [37], and longer reaction time).

To investigate the reason for this superiority, the Cu/Zn ratio of the optimized catalyst is compared with those of industrial catalysts [37] in Fig. 19. The Cu/Zn ratio of the optimized catalysts is apparently higher than those of industrial ones when compared with catalysts containing the same amount of Cu and Zn. Combining the result in Fig. 18 with that in Fig. 19, it can be said that the higher the Cu/Zn ratio is, the higher the activity is. This fact concurs with previous reports that the active site of Cu–Zn catalyst is metallic Cu, whereas Zn stabilizes Cu particles [28] and prevent their sintering [38]. That is, in a milder reaction condition, less Zn can stabilize the Cu particle to maintain its activity. The optimum Cu/Zn ratio, therefore, depends on the reaction conditions.

Reaction conditions should be different to develop a compact process of DME production based on a variety of carbon resources such as a small gas field, coal-bed methane, or biomass. Therefore, each process requires optimization because the Cu catalyst is very sensitive to reaction conditions. The combinatorial method can provide a useful tool for quick development of a tailor-made methanol catalyst and thereby accelerate process development.

5. Conclusion

This study performed simultaneous optimization of composition and preparation conditions of Cu–Zn–Al–Sc–B–Zr oxide catalyst for low-pressure methanol synthesis under mild (1 MPa, 498 K) reaction conditions using homemade combinatorial tools. Firstly, catalysts of random composition were prepared using an automated dispenser. Then their activities were measured in a high-throughput screening reactor system. These results were used as training data for an artificial neural network. In order to find the maximum point in the trained artificial neural network, a genetic algorithm was applied. Training data were selected from semi-optimized generation and appended for re-training of the network because the initial training data were insufficient for precise prediction. Finally, the optimum catalyst prepared using a 96 well microplate was summed up. Activity of the catalyst was measured in a conventional down flow fixed bed reactor to compare with conventionally developed catalyst.

Thus optimized catalyst using the retrained neural network consists of Cu/Zn/Al/Sc/B/Zr = 43/17/23/11/0/6 prepared using 2.2 times of oxalic acid and calcined at 605 K. The highest catalytic activity, 427 g-MeOH/kg-cat./h, was twice as high as that of industrial catalyst at 1 MPa, 498 K. The Cu/Zn ratio of the optimized catalyst was higher than those of industrial catalysts when the total content of (Cu + Zn) is equivalent. This higher ratio was considered to be suitable for reaction under lower temperature and lower pressure than with industrial conditions. The combinatorial tools developed here are useful to find optimal catalysts corresponding to reaction conditions.

Acknowledgements

We acknowledge financial support from Research for the Future Program of JSPS under the project “Synthesis of Ecological High Quality Transportation Fuels” (JSPS-RFTF98P01001) and from a Grant-in-Aid for the 21st Century COE project “Giant Molecules and Complex Systems” by the Ministry of Education, Culture, Sports, Science and Technology.

References

[1] A. Holtzwarth, P.W. Schmidt, W.F. Maier, Angew. Chem. Int. Ed. 37 (1998) 2644.
[2] B. Jandeleit, D.J. Schaefer, T.S. Powers, H.W. Turner, W.H. Weinberg, Angew. Chem. Int. Ed. 38 (1999) 2494.
[3] D. Wolf, O.V. Buyevskaya, M. Baerns, Appl. Catal. A 200 (2000) 63.
[4] O.V. Buyevskaya, D. Wolf, M. Baerns, Catal. Today 62 (2000) 91.
[5] K. Omata, G. Ishiguro, M. Yamada, Sekiyu Gakkaishi (J. Jpn. Pertol. Inst.) 43 (4) (2000) 317.
[6] A. Hagemeyer, B. Jandeleit, Y. Liu, D.M. Poojary, H.W. Turner, A.F. Volpe Jr., W.H. Weinberg, Appl. Catal. A 221 (2001) 23.
[7] S. Senkan, Angew. Chem. Int. Ed. 40 (2001) 312.
[8] J. Scheidtmann, P.A. Weiss, W.F. Maier, Appl. Catal. A 222 (2001) 79.
[9] U. Rodemerck, D. Wolf, O.V. Buyevskaya, P. Claus, S. Senkan, M. Baerns, Chem. Eng. J. 82 (2001) 3.
[10] O.V. Buyevskaya, A. Bruckner, E.V. Kondratenko, D. Wolf, M. Baerns, Catal. Today 67 (2001) 369.
[11] K. Omata, T. Umegaki, G. Ishiguro, M. Yamada, Sekiyu Gakkaishi (J. Jpn. Petrol. Inst.) 44 (5) (2001) 327.

[12] M. Richer, M. Langpape, S. Kolf, G. Grubert, R. Eckelt, J. Radnik, M. Schneider, M.M. Pohl, R. Fricke, Appl. Catal. B 36 (2002) 261.

[13] A. Corma, J.M. Serra, E. Argente, V. Botti, S. Valero, CHEMPHYSCHEM 3 (2002) 939.

[14] K. Omata, T. Umegaki, Y. Watanabe, M. Yamada, J. Jpn. Petrol. Inst. 45 (3) (2002) 192.

[15] T. Umegaki, K. Omata, G. Ishiguro, Y. Watanabe, M. Yamada, J. Jpn. Petrol. Inst. 46 (3) (2003) 181.

[16] K. Omata, T. Umegaki, Y. Watanabe, N. Nukui, M. Yamada, J. Jpn. Petrol. Inst. 46 (3) (2003) 189.

[17] C. Kiener, M. Kurtz, H. Wilmer, C. Hoffmann, H.-W. Schmidt, J.-D. Grunwaldt, M. Muhler, F. Schueth, J. Catal. 216 (2003) 110.

[18] T. Umegaki, Y. Watanabe, N. Nukui, K. Omata, Energy Fuels 17 (2003) 850.

[19] T. Hattori, S. Kito, Catal. Today 23 (1995) 347.

[20] Z.-Y. Hou, Q. Dai, X.-Q. Wu, G.-T. Chen, Appl. Catal. A 161 (1997) 183.

[21] K. Huang, F.-Q. Chen, D.-W. Lu, Appl. Catal. A 219 (2001) 61.

[22] K. Huang, X.-L. Zhan, F.-Q. Chen, D.-W. Lu, Chem. Eng. Sci. 58 (2003) 81.

[23] M. Holenă, M. Baerns, Catal. Today 81 (2003) 485.

[24] M. Holenă, M. Baerns, in: J.N. Cawse (Ed.), Experimental Design for Combinatorial and High Throughput Materials Development, Wiley–Interscience, New Jersey, 2003, Chapter 10, p. 163.

[25] V. Kecman, Learning and Soft Computing, MIT Press, London, 2001.

[26] K. Omata, Y. Watanabe, T. Umegaki, M. Hashimoto, M. Yamada, J. Jpn. Petrol. Inst. 46 (5) (2003) 328.

[27] R.G. Herman, K. Klier, G.W. Simmons, B.P. Finn, J.B. Bulko, T.P. Kobylinski, J. Catal. 56 (1979) 407.

[28] S. Fujita, Y. Kanamori, A.G. Satoriyo, N. Takezawa, Catal. Today 45 (1998) 241.

[29] Q. Sun, Y. Zhang, H. Chen, J. Deng, D. Wu, S. Chen, J. Catal. 167 (1997) 92.

[30] O.M. Busch, C. Hoffmann, T.R.F. Johann, H.-W. Schmidt, W. Strehlau, F. Schueth, J. Am. Chem. Soc. 124 (2002) 13527.

[31] K. Omata, Y. Watanabe, T. Umegaki, G. Ishiguro, M. Yamada, Fuel 81 (2002) 1605.

[32] K. Jun, W. Shen, K.S.R. Rao, K. Lee, Appl. Catal. A 174 (1998) 231.

[33] M. Kubo, K. Seki, C. Jung, T. Kusagaya, S. Takami, A. Imamura, A. Miyamoto, Shokubai 44 (6) (2002) 444.

[34] J. Wu, M. Saito, H. Mabuse, Catal. Lett. 68 (2000) 55.

[35] G.C. Chinchen, K.C. Waugh, D.A. Whan, Appl. Catal. 25 (1986) 101.

[36] K. Tohji, Y. Udagawa, T. Mizushima, A. Ueno, J. Phys. Chem. 89 (1985) 5671.

[37] K. Klier, Adv. Catal. 31 (1982) 243.

[38] K.C. Waugh, Catal. Lett. 58 (1999) 163.